Individual Pitch Control of A Clipper Wind Turbine for Blade In-plane Load Reduction

Shu Wang[1], Peter Seiler[1] and Zongxuan Sun[2]

***Abstract*— This paper proposes an H_∞ individual pitch controller for the Clipper C96 2.5 MW wind turbine installed at University of Minnesota. Different with existing results aimed to mitigate the blade out-of-plane loads, the proposed controller focuses more on reducing the blade in-plane loads. This is because the in-plane loads are dominating parts on the blade roots and therefore more critical to the life time of blades. To better balance the load reduction performance of different components on the turbine, the proposed controller takes the sum of filtered measurements of both blade in-plane and out-of-plane moments as feedback signals. It is expected to mitigate part of the in-plane periodic loads. Meanwhile, the high pass filtered measurements of the out-of-plane moments allow the controller to still mitigate high order harmonic terms of the out-of-plane loads. Therefore, the load reduction performance on the rotor shaft and nacelle should be improved. Simulation results show that the proposed design achieved these objectives.**

I. INTRODUCTION

Individual pitch control (IPC) has been widely accepted by modern wind turbines to mitigate rotation induced periodic loads on the turbine blades, shaft and nacelle [1], [2], [3], [4], [5], [6], [7]. Most of the existing results on IPC focused on reducing the blade out-of-plane moment [1], [5], [6], [7], considering that the failure would happen flapwisely somewhere on the blade and the flapwise load is more dependent on the out-of-plane moment. These designs had been proven to be effective by either high fidelity simulations [6], [7] or experiments [5]. By allowing higher bandwidth of actuation, these designs are also able to reduce periodic loads on the rotor shaft and nacelle, which are induced by higher order harmonics of blade out-of-plane motions.

However, the blade in-plane bending moment is also periodic and usually has larger variations than the out-of-plane bending moment. The in-plane periodic moment is mainly induced by gravity of the blade. Considering that the blade root is circular and connected to the hub with same bolts around the root, the in-plane periodic moments actually lead to larger damage equivalent loads (DELs) on the blade root and is therefore the dominating factor to the failure. In fact, IPC designs focused on reducing the out-of-plane moment might deteriorate the in-plane moment. It is therefore more meaningful to reduce the in-plane load if the failure is more easily happened on the blade root.

Reducing the in-plane loads relies on IPC to vary the aerodynamic moment on the blade and counter the gravity induced bending moment. However, there are two facts that could potentially limit the effect of this actuation. First, periodic components of the in-plane and out-of-plane bending moments are coupled with respect to the rotor azimuth angle. The IPC command aimed to counter the gravity induced in-plane moment will also lead to an extra periodic component to the out-of-plane moment. The resulting total out-of-plane moment might have larger variations. Second, the available aerodynamic moment to counter the gravity induced bending moment is limited, especially when the wind speed is slightly above Region 2. Even at higher wind speeds, the gravity induced periodic load can not be fully compensated.

To better balance the load reduction performance on the Clipper C96 $2.5\,\mathrm{MW}$ turbine installed at University of Minnesota, an H_∞ individual pitch controller that focuses more on the in-plane periodic load reduction is proposed in this paper. This controller takes the sum of filtered measurements of both blade in-plane and out-of-plane moments as feedback signals. It is expected to mitigate part of the in-plane periodic loads, which are dominating components at blade roots. Meanwhile, the high pass filtered measurements of the out-of-plane moments allow the controller to still mitigate high order harmonic terms of the out-of-plane loads. Therefore, the load reduction performance on the rotor shaft and nacelle should be improved. Simulation results show that the proposed controller achieved the design objectives.

The remainder of the paper is organized as follows. Section II provides some background knowledge on the turbine to be studied and the classic Multi-Blade Coordinate Transformation. Physical sources of the blade in-plane and out-of-plane loads and their effects are also analyzed in this section. Limitations of the IPC for in-plane load reduction are described in Section III. Details on the H_∞ IPC design and high fidelity simulation results are presented in Section IV and Section V, respectively. Section VI makes a brief conclusion of this paper and future work.

II. BACKGROUND

A. Clipper C96 Wind Turbine

The specific model that will be studied in this paper is the Clipper Liberty C96 wind turbine. This turbine, shown in Figure 1, is installed at the University of Minnesota UMore Park campus. This is an up-wind, utility-scale, three-bladed wind turbine with a rated power of $2.5\,\mathrm{MW}$. It is owned by the EOLOS Wind Energy Research Consortium at University of Minnesota [8]. The hub height of the turbine is $80\,\mathrm{m}$ and the rotor radius is $48\,\mathrm{m}$. Currently, a classic baseline controller similar to the designs in [9], [10], [11] is running

[1]S. Wang and P. Seiler are with the Department of Aerospace Engineering and Mechanics, University of Minnesota, emails:wang2927@umn.edu, seiler@aem.umn.edu. [2]Z. Sun is with the Department of Mechanical Engineering, University of Minnesota, email:zsun@umn.edu

on the turbine. Specifically, the torque control in Region 2 is applied for wind speeds from $4\,\mathrm{m/s}$ to $9\,\mathrm{m/s}$. The collective pitch control in Region 3 is applied for wind speeds from $12\,\mathrm{m/s}$ to $25\,\mathrm{m/s}$. A transition mechanism is used to switch between Region 2 and Region 3, when the wind speed is between $9\,\mathrm{m/s}$ and $12\,\mathrm{m/s}$. For protection of intellectual properties, the detailed structure and parameters of this baseline controller will not be shown in this paper.

Fig. 1. The Clipper C96 wind turbine at University of Minnesota

B. Multi-Blade Coordinate Transformation

The MBC transformation [12] is defined by a transformation matrix $T : \mathbb{R} \to \mathbb{R}^{3\times 3}$ as a function of the rotor position ψ:

$$T(\psi) = \frac{2}{3}\begin{bmatrix} \frac{1}{2} & \frac{1}{2} & \frac{1}{2} \\ \cos(\psi) & \cos(\psi+\frac{2\pi}{3}) & \cos(\psi+\frac{4\pi}{3}) \\ \sin(\psi) & \sin(\psi+\frac{2\pi}{3}) & \sin(\psi+\frac{4\pi}{3}) \end{bmatrix} \quad (1)$$

For a given rotor position ψ, $T(\psi)$ transforms variables associated with 3 blades from the rotating frame to the non-rotating frame. Conversely, the inverse of $T(\psi)$ transforms variables from the non-rotating frame to the rotating frame.

The MBC transformation has a straight forward physical interpretation in the application of wind turbines. Consider the bending moment M_i^{out} acting on the i-th blade in the out-of-plane direction. Applying the MBC transformation to the moment $M^{out} = \left[\, M_1^{out} \;\; M_2^{out} \;\; M_3^{out} \,\right]^T$ results in the moment in the non-rotating frame as $M_{nr}^{out} = \left[\, M_{col}^{out} \;\; M_{cos}^{out} \;\; M_{sin}^{out} \,\right]^T$. The superscript nr denotes variables defined in the non-rotating frame. After the transformation, these variables have meanings in terms of rotor motion instead of individual blades. M_{col}^{out} is the collective moment that causes the rotor to bend as a cone. M_{cos}^{out} and M_{sin}^{out} are the moments resulting in rotor tilt and yaw, respectively [13].

The MBC transformation can also convert the periodic linear time varying (PLTV) model of the turbine from the rotating-frame to the non-rotating frame [12]. The resulting LTV model is 'weakly' periodic and an LTI model can be approximated by averaging state space matrices of the weakly PLTV system over one rotor period. This LTI model is of sufficient accuracy for control oriented design purposes.

C. Periodic Loads on The Turbine

The rotation induced periodic loads on the turbine are mainly caused by wind shear, tower shadowing and blades gravity. These physical sources have different effects on the turbine components, which are reviewed in this section.

Wind shear and tower shadowing lead to the wind speed variation with respect to the rotor position. As an example, Figure 2 shows the effect of vertical shear in the out-of-plane direction. Under the assumption of constant wind conditions, the induced variation of blade out-of-plane motion will be periodic with respect to the rotor azimuth angle and contribute to the blade out-of-plane bending moments. The cyclic out-of-plane moments on three blades also lead to the tilt and yaw motions on the rotor shaft and nacelle [1], [6]. Specifically, the 1P component of blade out-of-plane motion is mapped by MBC to the 0P (constant) motion in the non-rotating frame. This 0P motion also induces the 0P motion of the rotor shaft and nacelle, which is not important from the perspective of DEL. However, the 2P component is mapped to the 3P motion, which leads to undesired periodic loads on the rotor shaft and nacelle.

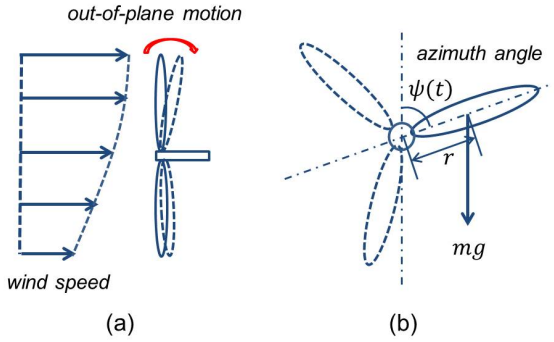

Fig. 2. Sources of periodic loads on the turbine

As shown in Figure 2(b), the gravity of blade induces an in-plane periodic bending moment with the rotor rotation. By taking the data of blade mass and the distance from the hub center to the blade mass center, the gravity induced in-plane moment of a single blade M_{1g} is calculated and plotted in Figure 3. In comparison, the time varying part of the in-plane moment of the same blade is also shown in Figure 3, by simulating the C96 turbine without IPC at a constant wind speed of Region 3. The vertical is set to 0.2 and the horizontal shear is 0. This time varying component is calculated by removing the mean value of the in-plane moment in the simulated time range. It is clear that the gravity induced periodic moment dominates the time varying part of the in-plane load and contributes to most of the DEL.

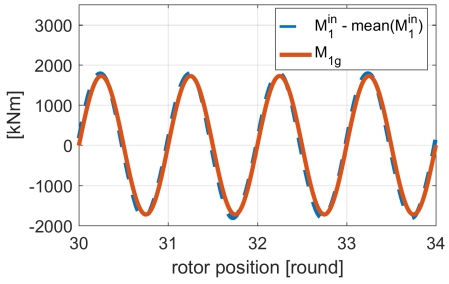

Fig. 3. The blade in-plane loads.

III. Limitations of IPC

Most of the existing results on IPC focused on reducing the blade out-of-plane moments [1], [6], [7]. Though these designs are effective, the IPC has minor effect on (or even degrades) the in-plane loads. As DELs on the blade roots are dominated by the in-plane moments, the life time of blades can be shortened with larger in-plane loads. Therefore, it is important to reduce the in-plane loads, which rely on IPC to vary the aerodynamic moment on the blade and counter the gravity induced bending moment. However, there are two facts that could potentially limit the effect of this actuation, which are explained in this section.

A. Loads Coupling

Figure 4 shows the FAST simulated out-of-plane and in-plane bending moments of a single blade in one round of rotation without IPC. The data is collected from the same simulation as described in Section II-C. It is seen that the in-plane and out-of-plane bending moments are different functions of the rotor angle. The IPC command aimed to counter the gravity induced in-plane moment will also introduce an extra periodic component on the out-of-plane moment. The resulting total out-of-plane moment might have larger variations. For the same reason, the IPC targets on out-of-plane load reduction might degrade the in-plane loads.

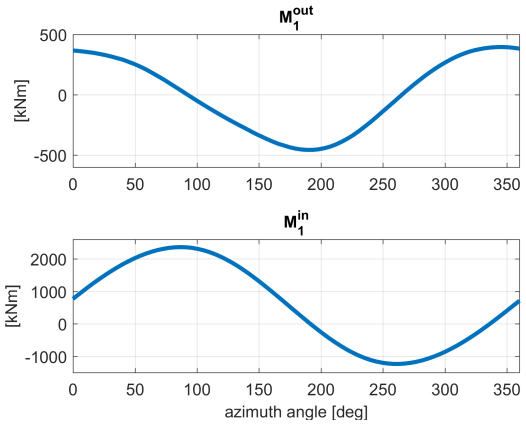

Fig. 4. The out-of-plane and in-plane loads in one period

It should be noted that the combination of in-plane and out-of-plane bending moments is a complex load on the blade root, which is time varying on both the magnitude and direction. Figure 5 plots this complex load on the 1-st blade root, denoted as $M_1(t)$, over 10 rounds of rotation. It is easily derived that $|M_1(t)| = \sqrt{(M_1^{out}(t))^2 + (M_1^{in}(t))^2}$. However, it should be clarified that $|M_1(t)|$ is not a valid metric to evaluate the load on the blade root, due to the direction variation of $M_1(t)$. Instead, as the in-plane projection of $M_1(t)$ has the most magnitude variation, it is reasonable to focus the load reduction in the in-plane direction.

B. Limited Aerodynamic Moment

Another factor that limits the potential of in-plane load reduction is the available aerodynamic moment. The in-plane

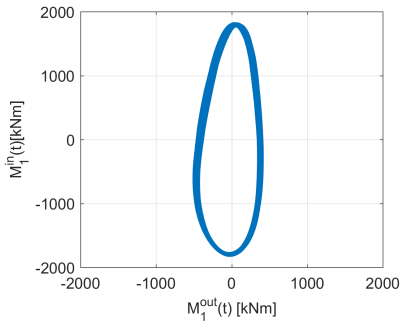

Fig. 5. The combined load $M_1(t)$ over 10 rounds of rotation

aerodynamic moments on the blades generate the torque on the rotor shaft, which can be calculated using the power coefficient C_p and other known parameters, such as nominal wind speed, rotor radius and rotor speed [10]. As a result, C_p and the available in-plane aerodynamic moment M_{1aero} on a single blade are all functions of the blade pitch angle β, as plotted in Figures 6. The left column of Figures 6 shows these functions at the wind speed of $12\,\mathrm{m/s}$ and the right column is for $20\,\mathrm{m/s}$. The nominal operation point of the turbine are denoted by circles on these curves. To maintain the normal operation of the turbine, the variation of M_{1aero} must be symmetric around the nominal point. It is noted that C_p at $12\,\mathrm{m/s}$ is very close to its maximum value. Therefore, M_{1aero} can only vary in a small range (around ± 100 kNm). The available M_{1aero} for IPC actuation generally increases with the wind speed. At the wind speed of $20\,\mathrm{m/s}$ (right column), however, the available variation of M_{1aero} (around ± 800 kNm) is still not enough to fully compensate the gravity induced in-plane moment, which is around ± 1800 kNm. It can be concluded that the IPC actuation is only capable of mitigating a portion of the in-plane loads.

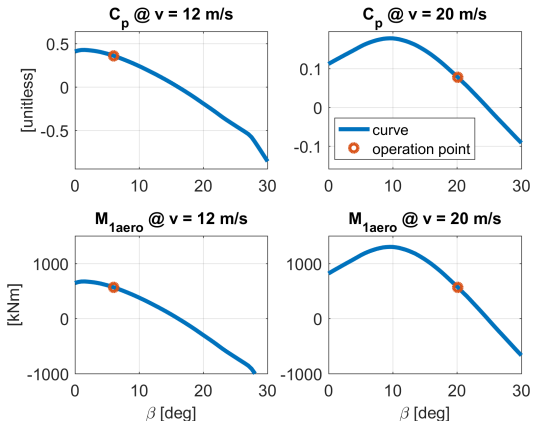

Fig. 6. C_p and M_{1aero} at different wind speeds

IV. Control Design

A. Control System Architecture

In this section, an individual pitch controller that focuses more on the in-plane load reduction is proposed. The block

diagram of the closed loop system is shown in Figure 7.

The plant for IPC design, denoted as P and shown in the dashed box of Figure 7, involves the interconnection of the turbine model G and the baseline controller K_b. In Region 3, K_b provides only the collective pitch control. The input to G is the cyclic pitch angle $\beta_{cyc} := \left[\begin{smallmatrix}\beta_{cos} & \beta_{sin}\end{smallmatrix}\right]^T$. The output of G include the cyclic in-plane moment $M^{in}_{cyc} := \left[\begin{smallmatrix}M^{in}_{cos} & M^{in}_{sin}\end{smallmatrix}\right]^T$ and the cyclic out-of-plane moment $M^{out}_{cyc} := \left[\begin{smallmatrix}M^{out}_{cos} & M^{out}_{sin}\end{smallmatrix}\right]^T$.

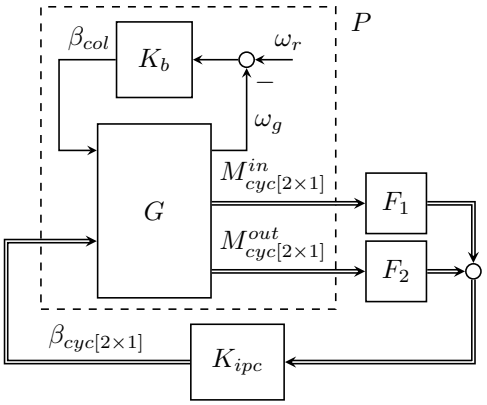

Fig. 7. The closed loop control system

The controller K_{ipc} takes the sum of filtered measurements M^{in}_{cyc} and M^{out}_{cyc} as feedback. Specifically, M^{in}_{cyc} is first low pass filtered through $F_1(s) = 0.015\frac{0.1}{s+0.1}I_2$. Therefore, only 0P component of the cyclic in-plane load is considered for mitigation through IPC. This load corresponds to the 1P component of the in-plane moment in the original rotating frame. As mentioned in Section III, reducing the in-plane load would potentially increase the out-of-plane load and the available in-plane aerodynamic moment is limited to fully mitigate the in-plane load. Therefore, the coefficient of F_1 is selected as 0.015, which scales the measurement down to $1.5\,\%$. In words, the controller K_{ipc} is expected to mitigate only part of the in-plane load. In practice, the coefficient and bandwidth of F_1 can be tuned for other trade-offs.

Meanwhile, M^{out}_{cyc} is high pass filtered through $F_2(s) = \frac{s+0.01}{s+0.1}I_2$, i.e. the high frequency components of M^{out}_{cyc} will be used as feedbacks for IPC. The bandwidth of F_2 is selected as $0.1\,\mathrm{rad/s}$, which is far away from the 3P frequency. Therefore, the 3P component of M^{out}_{cyc}, which corresponds to 2P terms of M^{out} in the rotating frame, can still be mitigated through IPC. This actuation will not significantly decrease the DEL of blade out-of-plane moments. Instead, the out-of-plane DEL, which is dominated by the 1P component in the rotating frame, might increase due to the low frequency actuation for in-plane load reduction. However, it should be noted that reducing the 3P component of M^{out}_{cyc} will be helpful to mitigate the blade out-of-plane motion induced 3P loads on the rotor shaft and nacelle. Similar to F_1, the filter F_2 can also be tuned in practice.

To summarize, the controller K_{ipc} targets on the 1P component of M^{in} (rotating frame) and the 3P loads on the rotor shaft and nacelle. As a compromise, M^{out} might increase. However, this trade-off should be acceptable if the DEL of M^{out} is lower than the DEL of M^{in}. More details on the plant model construction and the controller design will be provided in the following contents.

B. Linear Plant Model

The original turbine model is a high fidelity nonlinear model that includes aerodynamics and structural dynamics of the turbine drive train, tower and blades. This model is also provided by Clipper and is used in the Fatigue, Aerodynamics, Structures, and Turbulence (FAST) software [14] for simulation and control design purposes. FAST can linearize the turbine model at specific trim wind conditions. The linearization yields a PLTV system due to the rotor rotation. A 'weakly' PLTV system is obtained using the MBC transformation followed by averaging the state matrices [14]. This process yields an LTI model with sufficient accuracy.

In this paper, the LTI model G is generated at the trim wind speed of $12\,\mathrm{m/s}$. The linearization enables 9 degrees of freedom (DOFs) that include the rotor position, first tower fore-aft and side-to-side bending modes, and first flapwise and edgewise bending modes for each blade. The linearized model therefore contains 18 states. To avoid numerical issues in the control synthesis, the state of rotor position is removed and the resulting LTI model has 17 states.

The interconnection of G and K_b leads to an LTI plant P. It should be noted that P is further normalized for IPC design. Specifically, the channels from from β_{cyc} to M^{in}_{cyc} are normalized such that diagonal elements of the DC-gain matrix are equal to 1 and the same approach is applied to the channels from β_{cyc} to M^{out}_{cyc}.

C. H_∞ Control Design

The H_∞ control algorithm in the Matlab Robust Control Toolbox [15] is used in this paper to synthesis the individual pitch controller K_{ipc}. The objective is to find out a K_{ipc} that minimize the H_∞ norm of the augmented system, as shown in Figure 8. The classic loop-shaping technique is applied here to tune K_{ipc}. Specifically, 4 weighting functions W_n, W_d, W_e and W_u are included in the augmented system to specify design objectives. The principle on how to select these weights follows the experience in prior works [6], [7] and is briefly described here.

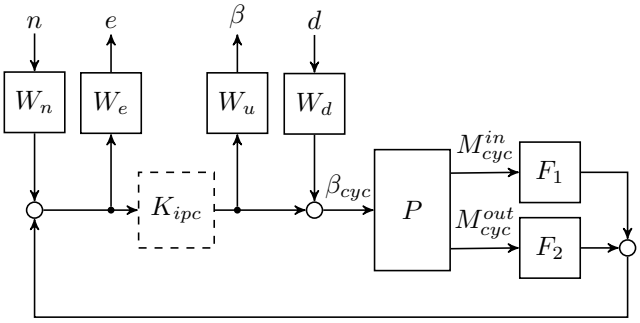

Fig. 8. The augmented system for control synthesis

W_d is the weight used to model the disturbance to the cyclic blade pitch input. It represents the wind turbulence

induced disturbance on pitch angles and has a significant effect on the structural loads. As load reduction is the main concern in the control design, it is selected as $W_d = I_2$. Another input weight W_n models the sensor noise to the controller K_{ipc}. In this design, it is assumed that the sensor noise has less effect to the system than the wind disturbance. Therefore, the weight is set as $W_n = 0.1I_2$.

The weights W_e and W_u are specified as follows:

$$W_e(s) = \frac{0.08s + 0.24}{s + 0.03}\frac{s^2 + 6.93s + 24}{s^2 + 0.49s + 24}I_2,$$
$$W_u(s) = 800\frac{s + 3.64}{s + 3640}I_2. \tag{2}$$

Here, W_e penalizes the frequency response of the load measurements. It is selected to limit the low frequency components with less emphasis on high frequencies. Therefore, the low frequency gain of W_e is 8 and the bandwidth is at around $0.2\,\mathrm{rad/s}$. This choice for W_e is expected to suppress the 0P component of M^{in}_{cyc}. It is noted that an inverse notch filter is also included in the expression of W_e to penalize the 3P component of M^{out}_{cyc}, which is at around $4.8\,\mathrm{rad/s}$. The weight W_u is selected as a high pass filter to penalize the cyclic pitch actuation, especially at high frequencies. The bandwidth of W_u is therefore selected at around $5\,\mathrm{rad/s}$, which is below the bandwidth of the C96 turbine pitch actuator (around $15\,\mathrm{rad/s}$). To ensure enough robustness, the low frequency gain of W_u is close to 1.

V. Simulation Results

To verify the load reduction performance of the proposed individual pitch controller, K_{ipc} is simulated in the FAST environment at various wind conditions.

In the first part, K_{ipc} is simulated at constant wind speeds. Here, the FAST simulation results are shown in Figure 9 for a constant wind speed at $20\,\mathrm{m/s}$, with a vertical shear of 0.2. K_{ipc} is compared with the baseline controller, which does not provide the IPC. Figure 9 provides the time series plots of 4 loads on the turbine in a $20\,\mathrm{s}$ frame, after the system goes to steady state. These loads include the 1-st blade in-plane moment M^{in}_1 and out-of-plane moment M^{out}_1, the rotor shaft tilt moment M_y and yaw moment M_z.

It is seen from the upper-left subplot of Figure 9 that M^{in}_1 is dominated by the 1P component and K_{ipc} reduces its amplitude by around 15%. In contrast, the upper-right subplot shows that M^{out}_1, which is also dominated by the 1P component, increased by around 30%. However, the amplitude of M^{out}_1 is still much lower than M^{in}_1 with the IPC on. It is also noted that there is an obvious phase shift on M^{out}_1 when K_{ipc} is applied. As analyzed in Section III-A, the in-plane aerodynamic moment generated to reduce the in-plane periodic load will be coupled with an extra out-of-plane aerodynamic moment, which might not be able to counter the existing out-of-plane periodic load. Therefore, the sum of all periodic terms at the out-of-plane direction might increase with a phase shift, as shown in the subplot. The loads for the 2nd and 3rd blades are similar to the results for the 1st blade and are therefore not shown here.

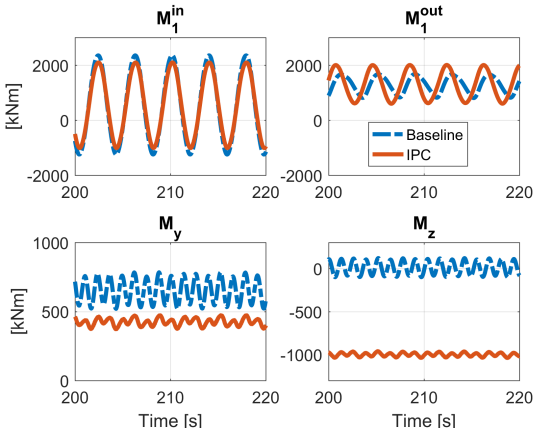

Fig. 9. Simulation results at $20\,\mathrm{m/s}$ constant wind speed

The rotor shaft tilt moment M_y and yaw moment M_z are shown in the lower-left and lower-right subplot of Figure 9. It is noted that the mean values for M_z and M_y change with K_{ipc} applied. However, the constant part of the load does not affect the DEL and is therefore not important for analysis. With only the baseline controller, M_z and M_y are dominated by 3P components, which are induced by cyclic out-of-plane motions of the blades. As a comparison, K_{ipc} significantly decreases the 3P loads on the rotor shaft. The tilt and yaw moments on the nacelle are similar to M_y and M_z, respectively, and are therefore not shown here.

In the second part, K_{ipc} is simulated in turbulent wind conditions to further quantify the load reduction performance. TurbSim [16] is used here to generate turbulent wind profiles. The turbulence spectral model is the Kaiman model and the turbulence level is 5 %, which corresponds to mild turbulence in practice. The average wind speed ranges from 12 m/s to 24 m/s with an increment of 4 m/s, i.e. 4 wind speeds are used for simulations. At each specific wind speed, 10 turbulent wind profiles are generated using random seeds and all profiles last for 11 minutes. The simulation data is collected and processed by MCrunch [17] to calculate the DELs. To avoid the effect of initial response, however, the data collected in the first 1 minute is excluded from analysis.

DELs and load reduction effects on the blades are presented in Figure 10. The left column shows DELs of the in-plane moment M^{in} for the two controllers (upper-left subplot) and the percentage of load reduction by using the IPC (lower-left subplot). Subplots on the right column have the same layout for the out-of-plane moment M^{out}. For simplicity, DELs of M^{in} and M^{out} are averaged over the 3 blades. At each wind speed, the DEL is also aggregated over 10 simulations. It is noted that M^{in} without IPC does not have a strong tendency to increase with the wind speed. This is because the in-plane load is dominated by the gravity induced moment, which is independent of the wind speed. By using the IPC, M^{in} is reduced by 3 % at $12\,\mathrm{m/s}$. As the wind speed increases, the load reduction performance gets better (up to 16 % at $24\,\mathrm{m/s}$). This observation fits with the conclusion in Section III-B that the capability of IPC to reduce the in-

plane load increases with the wind speed. It is also noted that the out-of-plane load increases steadily with the wind speed. As expected, the out-of-plane load increases at all wind speeds (up to $41\,\%$ at $16\,\mathrm{m/s}$) by using the IPC. However, the overall DEL on the blade root should still be improved as the out-of-plane load is much lower than the in-plane load at all wind speeds. As discussed in Section IV-A, the trade-off between in-plane and out-of-plane load reduction can be balanced by tuning filters F_1 and F_2. For example, decreasing the DC-gain of F_1 and/or increasing the DC-gain of F_2 will shift the focus to out-of-plane load reduction.

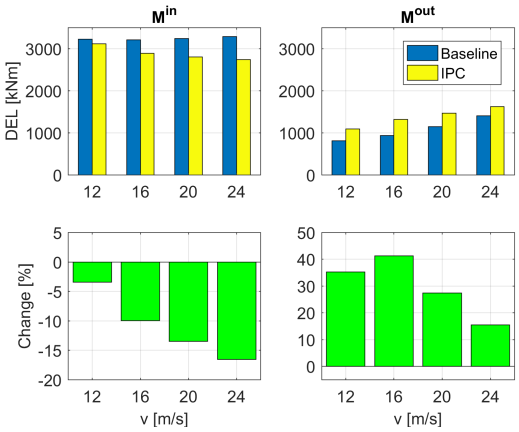

Fig. 10. DELs and load reduction on the blades

Figure 11 provides the load analysis results for the rotor shaft tilt moment M_y and yaw moment M_z, with the same layout as Figure 10. It is noted that the IPC reduces both loads by around $20\,\%$ at all wind speeds. This improvement can be attributed by mixing the high frequency out-of-plane load measurements at the feedback. Therefore, the control actuation can still actively suppress the out-of-plane motion induced 3P loads on the rotor shaft and nacelle. As the DELs on the nacelle are similar as on the shaft, the results are not shown here for limited space.

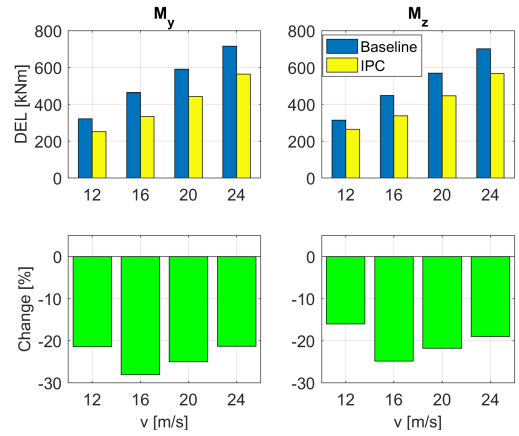

Fig. 11. DELs and load reduction on the rotor shaft

VI. CONCLUSION

This paper proposed an H_∞ design for individual pitch control of a Clipper C96 wind turbine. The proposed controller focuses more on reducing the in-plane periodic loads, which are dominating components on the blade roots and more critical to the life time of blades. By taking mixed sensor measurements of the in-plane and out-of-plane loads, this controller is able to mitigate the in-plane loads and the out-of-plane motion induced loads on the rotor shaft and nacelle. As a compromise, the blade out-of-plane loads will increase. The load reduction performance of the proposed design has been verified using high fidelity simulations. Future work will consider further limiting the out-of-plane load increase and implementing the control algorithm on the turbine for experiments.

VII. ACKNOWLEDGMENTS

This work was supported by Xcel Energy Renewable Energy Fund: No. RD4-13 *Virtual Wind Simulator with Advanced Control & Aeroelastic Model for Improving the Operation of Wind Farms* and National Science Foundation Grant No. NSF-CMMI-1254129 *CAREER: Probabilistic Tools for High Reliability Monitoring and Control of Wind Farms*.

REFERENCES

[1] E. A. Bossanyi, "Individual blade pitch control for load reduction," *Wind Energy*, vol. 6, no. 2, pp. 119–128, 2003.
[2] K. Stol and M. Balas, "Periodic disturbance accommodating control for blade load mitigation in wind turbines," *Journal of Solar Energy Engineering*, vol. 125, no. 4, pp. 379–385, 2003.
[3] A. Wright and M. Balas, "Design of controls to attenuate loads in the controls advanced research turbine," *Journal of Solar Energy Engineering*, vol. 126, no. 4, pp. 1083–1091, 2004.
[4] A. A. Ozdemir, P. J. Seiler, and G. J. Balas, "Performance of disturbance augmented control design in turbulent wind conditions," *Mechatronics*, vol. 21, no. 4, pp. 634 – 644, 2011.
[5] E. A. Bossanyi, P. A. Fleming, and A. D. Wright, "Validation of individual pitch control by field tests on two-and three-bladed wind turbines," *IEEE Transactions on Control Systems Technology*, vol. 21, no. 4, pp. 1067–1078, 2013.
[6] D. Ossmann, J. Theis, and P. Seiler, "Robust control design for load reduction on a Liberty wind turbine," in *ASME Dynamic Systems and Control Conference*, 2016, pp. Paper No. DSCC2016–9719.
[7] ——, "Load reduction on a Clipper Liberty wind turbine with linear parameter-varying individual blade-pitch control," *Wind Energy*, vol. 20, no. 10, pp. 1771–1786, 2017.
[8] "Eolos wind energy research consortium," http://www.eolos.umn.edu/.
[9] E. Bossanyi, "The design of closed loop controllers for wind turbines," *Wind Energy*, vol. 3, pp. 149–163, 2000.
[10] T. Burton, D. Sharpe, N. Jenkins, and E. Bossanyi, *Wind Energy Handbook*, 1st ed. John Wiley & Sons, 2001.
[11] J. Laks, L. Pao, and A. Wright, "Control of wind turbines: Past, present, and future," in *American Control Conference*, 2009, pp. 2096–2103.
[12] G. S. Bir, "User's guide to MBC3: Multi-blade coordinate transformation code for 3-bladed wind turbine," 2010.
[13] S. Wang, "Robust LPV control for wind turbines," Ph.D. dissertation, University of Minnesota, 2016.
[14] J. Jonkman and M. Buhl, *FAST User's Guide*, National Renewable Energy Laboratory, Golden, Colorado, 2005.
[15] G. Balas, R. Chiang, A. Packard, and M. Safonov, "Matlab robust control toolbox 3, users guide," 2010.
[16] B. J. Jonkman, "Turbsim user's guide: Version 1.50," 2009.
[17] J. M. Buhl, "MCrunch user's guide for version 1.00," May 2008, http://www.nrel.gov/docs/fy08osti/43139.pdf.